Inorganic Chemistry

pubs.acs.org/IC

Article

Mono-β-diketonate Metal Complexes of the First Transition Series

Claire E. Boronski, Sebastian M. Krajewski, Erin E. Sanchez, Michael P. Marshak,* and Aaron S. Crossman*

Cite This: *Inorg. Chem.* 2024, 63, 23158−23168

Read Online

ACCESS | Metrics & More | Article Recommendations | Supporting Information

ABSTRACT: Mono-β-diketonate compounds have been fleetingly observed in base metal catalyzed reactions, which are of current interest as alternatives to precious metal catalyzed reactions. Their isolation has been challenging due to synthetic and structural limitations of acac-type ligands, leading to the development of a related NacNac ligand platform. Herein we report the synthesis of a β-diketone capable of kinetically stabilizing relevant catalytic intermediates. Their efficient synthesis requires isolable acyl triflate and lithium enolate reactants. Further, the syntheses of several transmetalation salts are reported and used in transmetalation reactions with a series of late, first-row transition metal compounds (Fe^{II}, Co^{II}, Ni^{II}, Cu^{I}, Cu^{II}) of interest in base metal catalysis. In all, a dozen single-crystal XRD structures are reported, among other methods of characterization (i.e., IR, UV−vis, NMR, HRMS). The majority of the compounds present as mono-β-diketonate small-molecule bridged dimers. They serve as effective precatalysts and are accurately modeled by DFT calculations, validating the use of computational methods for determining structures and mechanisms. Their reactivity with various small molecules and solvents is also described. The utility of bis(2,6-dimesitylbenzoyl)methane (**L**) as a supporting ancillary ligand and a tool for further rational development of this class of ligands is discussed.

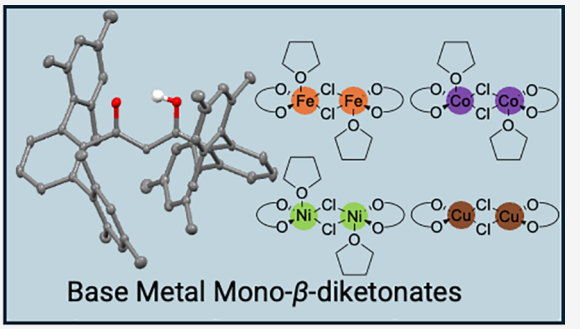

INTRODUCTION

Precious metal catalyzed reactions, such as the Suzuki,[1] Sonagashira,[2] and Buchwald−Hartwig[3,4] reactions, are the most utilized in organic synthesis and are often of choice in late-stage synthesis due to their high yield and reliability.[5−7] An important feature of these metal complexes is the steric hindrance of the supporting ligand—often involving N-, P-, and C-coordination centers—which protects the reactive metal center and promote low-coordinate reactive intermediates.[6,8−13] The kinetic stabilization of relevant intermediates has facilitated research into the mechanisms and led to the rational design of improved catalysts.[14−19] Due in part to the rising costs of precious metals,[20] there has been growing interest in base metal catalysis as an alternative for these essential reactions.[10,21−26] However, the less expensive base metals often display erratic yields unsuitable for late-stage synthetic applications.[5,6] Nonetheless, base metal catalyzed reactions involving β-diketonate supporting ligands continue to be explored as possible low-cost alternatives to precious metal catalysts.[27−35]

β-Diketonates are among the most well studied classes of ligands,[38,39] and they are particularly well-suited to the base metals due to their unique place within the spectrochemical and nephelauxetic series (Figure 1).[40−42] Specifically, β-diketonates promote delocalization of *d*-electrons through the pi system, while minimally perturbing the sigma interactions with the d-orbitals, thus forming tightly chelated, high-spin coordination compounds. However, it has been difficult to reap the same benefits of steric encumbrance within the class of β-diketonate ligands for two reasons: (1) the practical challenge of preparing sterically hindered examples; (2) functionalization being directed away from the coordinating atoms.[43] Therefore, isolating relevant catalytic intermediates and rationally designing improved catalysts remains elusive.[26,44−47] Consequently, many mechanisms catalyzed by these base metal catalysts remain unclear. As an example, there are at least five competing mechanistic proposals for Ullmann-type couplings—a versatile carbon bond forming reaction that has attracted much research interest.[32,48−53] Therefore, methods for preparing still more sterically encumbered ligands for catalytic studies remains desirable.

Claisen-type condensations[29] are the most common method of preparing β-diketonates but have a limited steric scope that has rarely exceeded dipivaloylmethane (dpm).[54,55] This limitation eventually led to the development of the N-coordinative NacNac motif half a century ago[56−61]—a structurally related class of supporting ligands that continues

Received: August 15, 2024
Revised: October 30, 2024
Accepted: November 7, 2024
Published: November 20, 2024

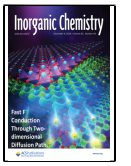

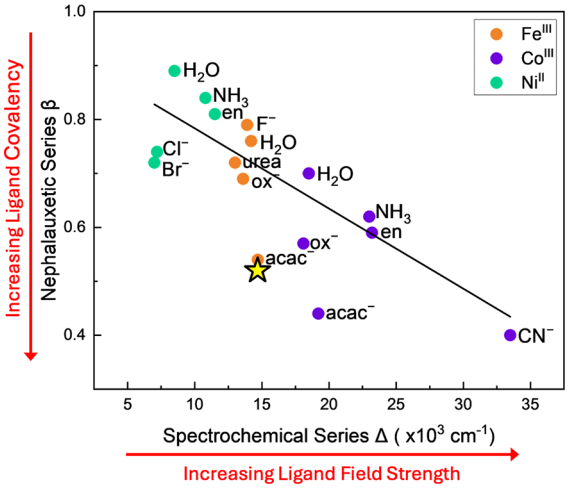

Figure 1. Nephelauxetic ratio ($B/B_{free\text{-}ion}$) and spectrochemical series of common homoleptic M^{III} (M = Fe, Co, Ni) complexes with various ancillary ligands.[36,37] The linear regression shows that the two series typically have an approximately linear relationship and that acac is an outlier. The yellow star marks the calculated values of $[Ni^{II}(\mathbf{L})(THF)(H_2O)(\mu\text{-}Cl)]_2$ **14**.

to flourish.[9,10,62−65] However, it is desirable to achieve a similar steric profile via an O-coordinative platform due to differences in catalytic behavior.[9,66−68] Previously, work in this laboratory demonstrated that acid chlorides can be used to expand the scope of Claisen-type condensations, specifically as the steric congestion around the reactive atoms increases, resulting in an improved yield of dpm and the modular introduction of *m*-terphenyl groups.[43,69] Eventually, the inadequacy of *m*-terphenoyl chlorides in the most challenging condensations necessitated the synthesis and isolation of *m*-terphenoyl triflates,[70] a notably potent acylating functional group.[71]

Herein we report a series of late first-row transition metal mono-*β*-diketonates lacking strong field supporting ligands. These suspected and fleeting catalytic intermediates are fully characterized, and some preliminary catalytic experiments of iron (C−C bond-forming Kumada−Tamao−Corriu reaction) and copper (C−O Ullmann reaction) are also disclosed. These exotic coordination motifs are enabled by the first *β*-diketone bearing two *m*-terphenyl groups. The necessary modifications to the Claisen condensation reaction for this steric regime are described as are several transmetalation salts useful for the preparation of transition metal complexes. Lastly, DFT models were calculated and shown to be in agreement with the crystallographic data collected.

RESULTS AND DISCUSSION

Synthesis of Bis-*m*-terphenyl *β*-Diketonates. The synthesis of bis(2,6-dimesitylbenzoyl)methane (**L**) is depicted in Scheme 1. The synthesis of 2,6-dimesitylbenzoyl triflate **4**, itself prepared from the corresponding acid chloride **1**, has been previously reported.[69] The enolate was prepared in two steps from acid chloride **1**. An excess (3 equiv) of MeMgBr, 3 M, was added to a solution of **1** in THF and refluxed for 16 h. The reaction was quenched with a minimal amount of water, followed by aqueous HCl and ethanol. The methyl ketone **2** was filtered from the biphasic mixture in excellent yield. This ketone was then enolized with a slight excess of *n*-BuLi, 2.5 M (1.05 equiv) in refluxing benzene, and removal of solvent afforded powdered enolate **3** in 77% yield. Surprisingly, no

Scheme 1. Synthesis of H(L) via Acyl Triflate 1 and Lithium Enolate 4 in DCM

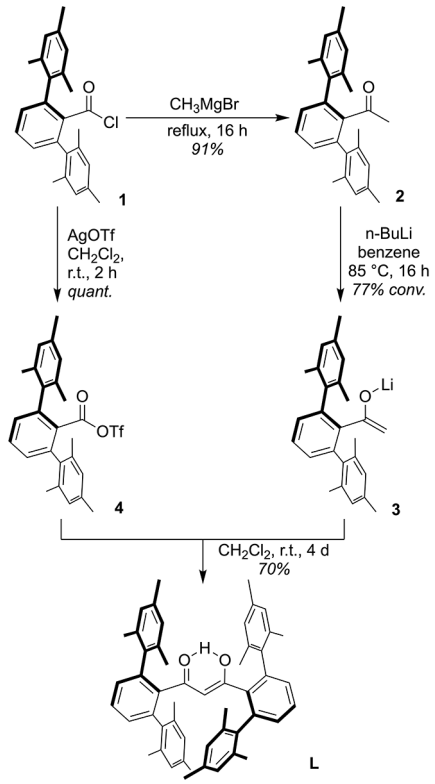

trace of tertiary alcohol was detected in either reaction, attesting to the steric protection provided by the *m*-terphenyl group. The remainder of the ketone was present in the crude powder of **3** and was recovered after subsequent condensation. The extent of enolization was determined by ^{1}H NMR, and the appropriate amount of acyl triflate **4** was slurried with crude **3** in DCM and stirred for 4 days at room temperature. The low temperature was required as heating the reaction mixture results in intramolecular acylation of a mesityl ring with concomitant methyl group migration.[70] A crude mixture of H(**L**) and residual ketone **2** is obtained in 70% yield after workup. The product can be separated by refluxing with KOH in 2:1 hexane/toluene and filtering the ketone from a solution of potassium *β*-diketonate. Recovered ketone **2** can be used in subsequent condensations for a more efficient overall synthesis. Notably, the equivalent magnesium and sodium enolates result in considerable O-acylation byproduct that cannot be easily separated. Up to 50 g lots of **L** have been prepared using these procedures. A single crystal of the protonated ligand was also analyzed by XRD, revealing a monomeric enolic isomer with C_2-symmetry about the H−C_α axis (Scheme 2).

Initial Metalation with Li, K, and Tl. It was deemed advantageous to have several options for the transmetalation reactions. Therefore, salts of Li, K, and Tl[1] were prepared (Scheme 2). Highlighting the improved durability of **L** toward strong nucleophiles, reaction of H(**L**) with *n*-BuLi, 2.5 M, resulted in a dark green solution that slowly faded to red and afforded the product in 89% yield. ^{1}H NMR indicated that there were no coordinated THF molecules, leading to the tentative assignment as $[Li(\mathbf{L})]_2$ (vide infra). During several crystallization attempts, this material slowly and reversibly decolorized upon scavenging THF in the glovebox to yield the

https://doi.org/10.1021/acs.inorgchem.4c03477
Inorg. Chem. 2024, 63, 23158−23168

Scheme 2. Syntheses of the Li, K, and Tl Complexes of L[a]

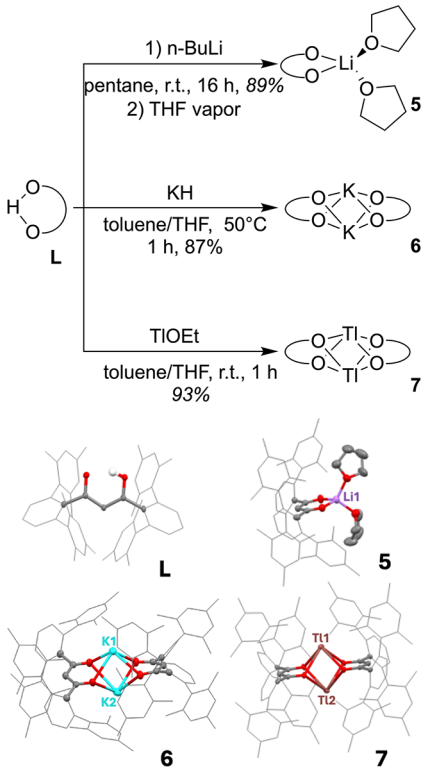

[a]Also shown are crystal structures of the **L** and **5**–**7**. Hydrogen atoms omitted for clarity, excepting the enolic proton. Thermal ellipsoids for the metal centers and chelate rings are drawn at the 50% confidence level.

red mono-THF bridged dimer $[Li(\mathbf{L})(THF)]_2$ and eventually the colorless monomeric $Li(\mathbf{L})(THF)_2$ **5**. Application of a high vacuum liberated the coordinated THF molecules. The bis-THF complex was also directly prepared in THF using *n*-BuLi, 2.5 M, in 67% yield and structurally characterized. Treatment of H(**L**) with KH or $Tl^{I}OEt$ in 1:1 THF/toluene yielded $[K(\mathbf{L})]_2$ **6** and $[Tl(\mathbf{L})]_2$ **7** in 87% and 93% yields, respectively. Single crystals of these complexes were grown and analyzed by XRD to ascertain their coordination geometries (Scheme 2). Both compounds showed interesting above-and-below dimeric structures where both metal atoms exhibited O_4-coodination spheres with weak associations with nearby mesityl rings. These materials were useful in subsequent metalation experiments given their range of chlorophilicities (Tl^{I} > K ∼ Li > H). In these and all other experiments using **L**, the ligand could be recovered from waste streams by acidification and extraction into toluene and then slurrying the crude organics into acetone, from which the ligand was filtered.

Crystallography of Fe, Co, Ni, and Cu. The later first transition series were chosen for initial studies using **L** owing to their relevance in carbon bond-forming reactions.[35,43] Each metal dichloride was reacted with $[K(\mathbf{L})]_2$ in THF. The Fe^{II}, Co^{II}, and Ni^{II} salts gave bridged compounds featuring an axially coordinated THF ligand per metal center in a trans configuration, $[M^{II}(\mathbf{L})(THF)(\mu\text{-}Cl)]_2$ (M = Fe **8**, Co **9**, Ni **10**) (Scheme 3). $Cu^{I}Cl$ reacted slowly with the potassium salt, but when stirred with $[Tl(\mathbf{L})]_2$ immediately gave complex $[Cu(\mathbf{L})]_2$ **16** (Scheme 3). Other derivatives could be synthesized by treating these compounds with heat, vacuum, other solvents, or atmosphere; see the Supporting Information for detailed syntheses. Given that these structures closely resembled putative and fleeting reactive intermediates, their crystallographic analyses were prioritized (Figure 2). Eight of these compounds were characterized by single-crystal XRD, and all but one were bridged dimers. The steric bulk of **L** resulted in considerable strain in ML_2-type structures, and this strain was much reduced in the dimers bridged by small molecules. To guide the discussion of this unusual coordination behavior, bond lengths, angles, and geometric indices[72,73]—commonly used indicators of steric strain in metal complexes—were often referred to (Table 1).

Iron. The dimer $[Fe^{II}(\mathbf{L})(THF)(\mu\text{-}Cl)]_2$ **8** crystallized as a pentacoordinate complex. The coordinated THF molecules were not removed with application of heat or high vacuum. When comparing the M–Cl bond lengths, one bond was 0.17 Å longer than the other, suggesting an unequal electron donation from each chloride to the two metal centers. Also noteworthy, the Fe^{II} centers were observed to be between a square pyramidal and a trigonal bipyramidal geometry (τ^5 =

Scheme 3. Synthesis of Late First-Row Transitional Metal Complexes of L (M = Fe^{II}, Co^{II}, Ni^{II}, Cu^{II}, and Cu^{I})

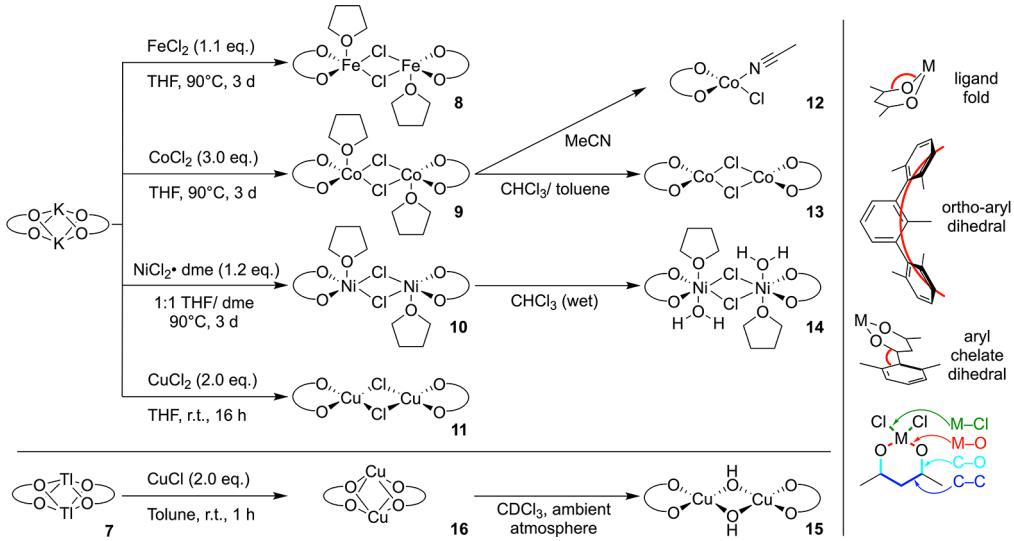

https://doi.org/10.1021/acs.inorgchem.4c03477
Inorg. Chem. 2024, 63, 23158–23168

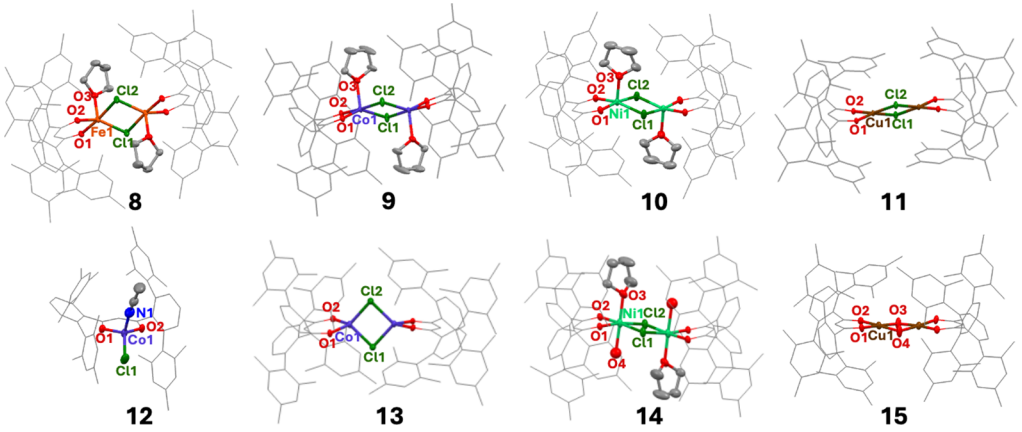

Figure 2. Crystal structures for the new metal β-diketonates are described. Thermal ellipsoids (50%) are shown for the chelate rings and phosphorus atoms. Hydrogen atoms and solvent molecules were removed for clarity. Unabridged structures can be found in Figures S5–S12.

Table 1. Average Bond Angles, Lengths, And Geometric Indices Calculated from the scXRD Structures

	Angles (°)			Lengths[a] (Å)				Geometric Indices	
Complex	Fold	Ortho-aryl dihedral	Aryl-chelate dihedral	M–O	C–O	C–C	M–Cl	τ_5	τ_4
Fe^{II} **8**	2.06	132.27	56.47	1.989	1.274	1.404	2.349	0.51	
		145.72	62.88	2.121			2.516		
Co^{II} **9**	0.5	143.795	63.96	1.974	1.276	1.402	2.306	0.55	
			58.31	2.071			2.494		
Co^{II} **13**	5.01	137.54	63.03	1.896	1.292	1.4055	2.2975		0.78
	0.68	126.63	49.6	1.911	1.273				
Co^{II} **12**	9.12	147.87	64.11	1.942	1.283	1.394	2.219		0.92
		149.75	54.73						
Ni^{II} **10**	6.85	147.75	61.88	1.996	1.263	1.3995	2.353	0.15	
		136.36	67.23	2.197	1.273				
Ni^{II} **14**	16.78	147.78	68.89	2.023	1.2715	1.410	2.377		
		134.53	59.91	2.197					
Cu^{II} **11**	13.64	125.505	66.5	1.895	1.283	1.402	2.282		0.28
Cu^{II} **15**	3.6	133.09	71.01	1.895	1.272	1.396			0.096
			59.33						
Cu^{II} **17**	0	134.21	55	1.928	1.282	1.397			0.05

0.51). Also noteworthy, the ortho-mesityl ring dihedral angles deviated significantly from ideal 120° to 132° and 145°, and the fold angle strain of 2° deviated from the ideal null. Our hypothesis was that crystal packing effects were mainly responsible for the observed angle strain in the β-diketonate ligand. Previous work in this laboratory showed that bond angles could display a great deal of flexibility in similar metal β-diketonates, whereas bond lengths were notably consistent.[32]

Cobalt. Similar to the iron complex **8**, metalation with $CoCl_2$ gives the chloride-bridged dimer $[Co^{II}(\mathbf{L})(THF)(\mu\text{-}Cl)]_2$ **9** featuring axially coordinated THF ligands. The dimer could be disrupted by recrystallization from acetonitrile to give the first reported monomeric mono-β-diketonate species lacking strong field ligands characterized by XRD, among other techniques, as $Co^{II}(\mathbf{L})(Cl)(MeCN)$ **12**. Unlike the iron complex, the THF ligands could be removed from the cobalt dimer by application of high-vacuum or by recrystallization from chloroform/toluene to give $[Co^{II}(\mathbf{L})(\mu\text{-}Cl)]_2$ **13**, indicating reversibility of THF coordination. All three demonstrate the tendency of Co^{II} to achieve a tetrahedral geometry, as illustrated by the geometric indices for **9**, **12**, and **13**. The pentacoordinate dimer **9** with axial THF molecules shows a τ^5 of 0.55, an intermediate geometry similar to the iron analog. Also like the iron analog, the same dimer shows significant ortho-aryl dihedral strain that deviates from 120° to nearly 144° but also exhibits a small fold angle of 0.5°. On the other hand, the dimer lacking THF exhibits less strained ortho-aryl dihedral angles of 127° and 137°, but a higher fold angle strain of 5° and 0.7°. This pair of Co^{II} dimers exemplifies the balance struck between the optimal coordination geometry and ligand bulk strain. The Co^{II} monomer complex **12** has the greatest ligand fold and ortho-aryl dihedral distortions of the three at 9° and 151°, respectively, and also the shortest M–Cl bond length of the reported structures. These extreme distortions suggest a decreased importance of conjugation with the β-diketonate π-system and an increased interaction from the π-bonding electrons of electronegative MeCN and Cl^- ligands.

Nickel. The tendency to fold the chelate ring, thereby reducing the conjugation with the acac-type ligand, is even more evident with the two Ni^{II} complexes obtained. The complex $[Ni^{II}(\mathbf{L})(THF)(\mu\text{-}Cl)]_2$ **10** on average shows greater ligand fold angles (6.85°) and elongated M–THF and M–Cl bond lengths, thus reducing the electron density of the metal center. This highlights that β-diketonates such as **L** make these complexes extremely electropositive and promotes ionic interactions with electronegative atoms such as Cl and O. Like the Fe^{II} complex **8**, the THF ligands cannot be removed

https://doi.org/10.1021/acs.inorgchem.4c03477
Inorg. Chem. 2024, 63, 23158–23168

under a variety of conditions effective for Co^{II} complex **9**. Conversely, a dimeric nickel complex with coordinated water molecules, $[Ni^{II}(\mathbf{L})(THF)(H_2O)(\mu\text{-}Cl)]_2$ **14**, is obtained when recrystallized from wet chloroform, consistent with related compounds' tolerance to water.[74] The Racah parameter and octahedral crystal field ligand splitting values are calculated for **14** and further exemplify acac's propensity to form tightly chelated, high-spin complexes. The M−O and M−Cl bond lengths are longer in the hydrated compound than in **10**, and the structure shows an astonishing 16.8° ligand fold distortion, indicating deviation from the pseudoaromatic chelate ring formed in the other complexes. Both compounds also show exaggerated ortho-aryl dihedral angles to accommodate this congested ligand sphere.

Copper. Copper is particularly known for enforcing regular coordination geometry in β-diketonate compounds[75,76] and was used in our prior work as a platform for probing the steric demand of new ligands.[32] Metalation with $Cu^{I}Cl$ gave complex $[Cu^{I}(\mathbf{L})]_2$ **16**, displaying diamagnetivity per ^{1}H NMR studies (Figure S23). The lack of any supporting ligands suggests that the compounds could exist as another above-and-below dimer, analogous to the $[M(\mathbf{L})]_2$ (M = K, Tl^{I}) complexes. However, the presence of additional resonances in the ^{1}H NMR spectrum, particularly among the methyl groups, suggests that there could be additional speciation occurring. Despite several years of attempts, this compound has resisted crystallization. Nonetheless, its solutions have persisted for several weeks and can be used in catalytic studies, demonstrating that the increased steric bulk of the ligand increases kinetic stability compared to the short-lived parent Cu(acac) complexes.[47] Exposure of a solution of **16** in $CDCl_3$ to atmosphere results in crystals of $[Cu^{II}(\mathbf{L})(\mu\text{-}OH)]_2$ **15**, suggesting O_2 activation and H atom abstraction by the compound as seen in related NacNac complexes.[16] Lastly, heating **16** slowly results in a disproportionation reaction to give single crystals of $Cu^{II}(\mathbf{L})_2$ **17**, exhibiting square planar coordination geometry and significant ortho-aryl dihedral strain in the supporting ligands. The Cu^{II} bridged-chloride dimeric complex $[Cu^{II}(\mathbf{L})(\mu\text{-}Cl)]_2$ **11** is also isolated lacking supporting ligands. This complex shows another impressive fold angle of 13.6°, disrupting the conjugation among the chelate rings and chloride π-orbitals. Relative to the hydroxide-bridged dimer **15**, the chloride-bridged dimer **11** is somewhat distorted from square planar with a τ^4 geometric index of 0.28 and features the least strained *m*-terphenyl group. Complex **15** assumes a less strained coordination geometry indicated by a geometric index of 0.096, yet a more strained ligand configuration. We attribute this to the fact that the OH^- is higher on the spectrochemical series and therefore is a stronger field ligand than Cl^-, forcing the metal into a more rigid square planar geometry.

Isostructural Trends. The supporting β-diketonate ligand **L** promotes different coordination spheres/geometries and shows impressive flexibility. Notably, the ortho-aryl dihedral (idealized as 120°) and fold angle (idealized as 0°) are particularly flexible, ranging from 126−151° and 0.5−16.8° respectively. The geometric indices, τ^4 and τ^5, also illustrate the relative flexibility of the coordination sphere, as the metal center and ligand sphere are varied. This versatility permits the ancillary ligand **L** to promote exotic coordination chemistry among these base metals. Crystal packing effects may also contribute to these observed structural features, hence the need for solution-simulated computational studies of analogous parent acac-type metal complexes.

Computational Studies of Ligand Series. For comparison with the crystallographic data, DFT calculations were carried out for many of the disclosed metal complexes using the ORCA 5.0 package.[77] These models included $[M^{II}(acac)(THF)(\mu\text{-}Cl)]_2$, $[M^{II}(acac)(\mu\text{-}Cl)]_2$, and $M(acac)_2$ (M = Fe, Co, Ni, Cu) and $[M^{I}(acac)]_2$ (M = Li, K, Tl). Models were also prepared for $[Ni^{II}(acac)(THF)(H_2O)(\mu\text{-}Cl)]_2$ and $Co^{II}(acac)(MeCN)(Cl)$. As a reference, the $Cu(acac)_2$ crystal structure was available for comparison with the calculated structure and $Cu^{II}(\mathbf{L})_2$, whereas the Fe, Co, and Ni salts existed as oligomers in the crystal state.[78−80] The calculations were performed by using the B3LYP functional, the DEF2-TZVPP basis set, and the def2/J auxiliary basis set. The common use of acac in reactions and the significant savings in computation power motivated its use in these models, although some error was introduced by its use in place of **L**. Of many parameters available, differences in M−O, C−O, C−C, and M−Cl bond lengths were selected to focus the conversation. The results are summarized in Table 2.

Table 2. Calculated Bond Lengths Using the ORCA 5.0 Software Package[77] Using the B3LYP Functional and DEF2-TZVPP and def2/J Basis Sets

	Bonds	Fe	Co	Ni	Cu
ML_2	M−O	1.833	1.974	1.938	1.955
	C−O	1.300	1.273	1.270	1.280
	C−C	1.411	1.408	1.401	1.415
	M−Cl				
$[M(L)(\mu\text{-}Cl)]_2$	M−O	1.935	1.935	1.928	1.944
	C−O	1.275	1.275	1.271	1.280
	C−C	1.403	1.402	1.398	1.401
	M−Cl	2.341	2.341	2.316	2.327
$[M(L)(THF)(\mu\text{-}Cl)]_2$	M−O	2.029	1.997	1.988	1.945
	C−O	1.269	1.269	1.268	1.268
	C−C	1.404	1.403	1.403	1.400
	M−Cl	2.390	2.339	2.396	2.340

First, the accuracy of the models was determined to validate DFT as a tool to rationalize reaction mechanisms.[81,82] The percent error of calculations comparing the DFT and the experimental XRD data was determined for all parent-acac analogous structures (Supporting Information Table S90) and ranged from 1 to 3%, indicating that the calculated structures served as accurate models for the ligand platform. Therefore, the use of DFT models was justified for rationalizing reaction mechanisms more broadly as found in the literature, and the calculations extended to nonisolated compounds were deemed an accurate representation.

Comparison with NacNac Complexes. Historically, related compounds bearing NacNac ligands have been known and well-studied due to the ease of steric tuning for catalytic applications by modifying the N-substitution. Structurally related NacNac complexes selected for comparison can be described as $[M^{II}(NacNac)(\mu\text{-}Cl)]_2$ (M = Fe, Co, Ni, Cu), although they bear N-aryl rings that help promote their unique coordination environment. Most bear *N*,*N*-2,6-diethylphenyl groups,[63,83,84] except Ni, which bears *N*,*N*-2,6-dimethylphenyl groups.[85] Their XRD structures are very similar, with M−O and M−Cl bonds being slightly shorter by 1−2% due to the increased ionic character of metal−oxygen

https://doi.org/10.1021/acs.inorgchem.4c03477
Inorg. Chem. 2024, 63, 23158−23168

bonds relative to nitrogen (Table S91). The C−N bond is about 8% longer relative to the C−O bonds as well, while the C−C bonds are slightly shorter in the NacNac examples. These experimental results are also similar to the DFT calculations of related $[M(acac)(\mu\text{-}Cl)]_2$ (M = Fe, Co, Ni, Cu) described above. Therefore, the new acac-type ligand **L** represents a valuable parallel to well-established NacNac chemistry and a new generation of β-diketonates capable of promoting a similar coordination environment, importantly, with unique higher-spin coordination environments.

Catalytic Studies of Cu(I/II) and Fe(II) in C−X Bond Forming Reactions. Elucidating the mechanisms of these late, first-row transition metals is important for the development of the β-diketonate platform in light of the many contradicting mechanisms proposed for its cross-coupling reactions.[86−89] A sufficiently sterically hindered supporting ligand is required to facilitate such studies. Bis-*m*-terphenyl β-diketonates can stabilize the proposed catalytic intermediates, and their efficacy in cross coupling reactions with base metals highlights their relevance. Preliminary work in this direction is disclosed for an iron-catalyzed Kumada−Tamao−Corriu and a copper-catalyzed Ullmann cross-coupling reaction.

The Kumada−Tamao−Corriu coupling reaction is a carbon−carbon bond forming reaction between an aryl or alkyl Grignard-type nucleophile and a vinyl or aryl halide electrophile catalyzed by nickel or palladium.[90] Kochi discovered that ferric salts were effective transition metal catalysts for this coupling reaction.[91] Previous investigations in this lab into the mechanism of the Kumada coupling reaction using sterically hindered catalysts showed similar efficiency to $Fe(acac)_3$.[92] In the present work, precatalysts including $FeCl_3$, $Fe(acac)_3$, $Fe(dbm)_3$,[87,93] $[Fe(^{Ar}acac)(THF)_2]_2(\mu\text{-}OTf)_2$ ($^{Ar}acac$ = 2,6-Mes_2BzPin),[92] and $[Fe^{II}(\mathbf{L})(THF)(\mu\text{-}Cl)]_2$ **8** were screened in a model reaction (Scheme 4). Experimentally,

Scheme 4. Synthesis of Methyl 4-*n*-Hexylbenzoate via Kumada-Type Coupling Reaction

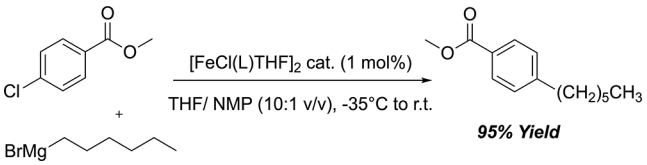

the reaction proceeded rapidly (i.e., <15 min), with complete conversion (by ^{1}H NMR) and mass balance with a 5 mol % catalyst loading with respect to Fe^{II}. No side products, such as additions to the ester, were observed. Slower apparent turnover rates were observed with **8** as the catalyst compared to $Fe(acac)_3$, which increased the reaction time. Thus, extremely hindered ligand **L** enabled isolation of relevant intermediates for future mechanistic investigations.

Both $[Cu^{I}(\mathbf{L})]_2$ and $[Cu^{II}(\mathbf{L})(\mu\text{-}Cl)]_2$ **10** were investigated as potential catalysts using a model reaction for the copper catalyzed Ullmann-type diaryl ether coupling reaction[94−97]—the formation of 2-phenoxynaphthalene (Scheme 5). Previous catalytic investigations have suggested the loss of a β-diketonate from the Cu^{II} precatalysts was a significant barrier to catalyst activation.[32] The bulky **L** supported precatalysts afforded the desired product at 90 °C after several days, and trace diaryl ether product was also observed by TLC at ambient temperature after 4 days. Supported by **L**, the Cu^{I} precatalysts afforded the best yields, while the Cu^{II} precatalysts

Scheme 5. Synthesis of 2-Phenoxynaphthalene via Ullmann-Type Coupling Reaction

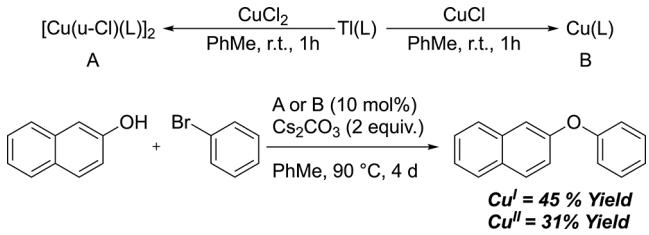

also performed well (see the Supporting Information). The slow deactivation of Cu^{I} was noted as an important side reaction. These results suggested that increasingly large ligands increased turnover number but decreased turnover rate, as demonstrated by the robustness and sluggishness of the **L**-supported precatalysts as compared to smaller β-diketonates. This observation was also in agreement with the common use of base metals in several mol % versus parts per million levels of precious metal precatalysts.

CONCLUSIONS

The most sterically hindered β-diketonate to date has been prepared and used to support the first reported series of isolated mono-β-diketonate salts of late first-row base metals of interest in sustainable catalysis. The supporting ligand's efficient, decagram synthesis utilizes an isolated acyl triflate and lithium enolate in the key bond-forming reaction. The proteoligand, three M^{I} salts, and eight M^{II} salts have been characterized crystallographically. Its salts have been used to gain insight into their structure and to verify their catalytic relevance (e.g., for iron [Kumada−Tamao−Corriu reaction] and copper [Ullmann reaction]). This ligand serves both as an ancillary ligand in catalysis and as a path forward in isolating reactive intermediates and rational development of catalytic reactions. The Li, K, and Tl^{I} salts serve as transmetalation agents for other metals for further studies. Although not crystalline, Cu^{I} was stable on the order of weeks rather than minutes. The M^{I} salts tend to present as unsupported, above-and-below the O_4-coordination plane dimers, whereas the M^{II} salts tend to present as small molecule bridged dimers. These examples finally bring acac into the level of steric encumbrance enjoyed by NacNac for half a century. Further, these are among the first isolable examples of what are otherwise elusive reactive intermediates in base metal catalyzed reactions. DFT models using the parent acac ligand for all crystallized M^{II} compounds and ML_2-type compounds were generated for comparison, finding good agreement between calculations and experimental data.

EXPERIMENTAL SECTION

Syntheses were performed in a nitrogen-filled glovebox or in a fume hood using standard air-free Schlenk techniques. Organic reagents were purchased from Alfa Aesar, TCI Chemical, or Sigma-Aldrich and used as received. Deuterated solvents were purchased from Cambridge Isotope Laboratories and stored over 4 Å molecular sieves. All other solvents were purchased in anhydrous form from Sigma-Aldrich and further dried with and stored over 4 Å molecular sieves. **1**[70] and **2**[98] were synthesized according to literature procedures. NMR spectra were recorded on a Bruker Avance-III 400 NMR spectrometer. Infrared spectra were recorded on an Agilent Cary 630 FTIR instrument with ATR attachment. UV−vis spectra were recorded on an Agilent Cary 60 UV−Vis Spectrophotometer using quartz cuvette

https://doi.org/10.1021/acs.inorgchem.4c03477
Inorg. Chem. 2024, 63, 23158−23168

with a 1 cm path length. Melting point was determined with a SRS Digimelt. Mass spectrometry data were collected on an Thermo-Scientific ISQ LT mass spectrometer. Magnetic data were collected in specified solvent solutions at room temperature using Evans' method.[99,100] The reported value is the mean of three separately prepared and measured solutions. Magnetic susceptibility data were corrected for diamagnetic contributions for the core diamagnetism of each sample (estimated using Pascal's constants). X-ray crystal structures were collected by using a Bruker D8 Quest Eco three circle goniometer platform equipped with a Bruker APEX-II CCD detector. A graphite monochromator was employed for wavelength selection of the Mo Kα radiation (λ = 0.71073 Å). The data were processed by using APEX III software provided by Bruker. The structures were solved by the methods noted below. Hydrogen atoms were placed in calculated positions by using the standard riding model and refined isotropically.

Synthesis of 2,6-Dimesitylacetophenone (3). To an oven-dried, nitrogen-filled 1 L round-bottom flask containing a PTFE-coated, magnetic stir bar, reflux condenser, and septum was added 2,6-dimesitylbenzoyl chloride **2** (50 g, 130 mmol). Anhydrous THF (260 mL) was cannulated through the condenser into the RBF followed by MeMgBr (111 mL, 3 M, 390 mmol). The solution refluxed at 60 °C for 16 h. An aliquot of the resulting dark red/brown solution was removed, quenched with 0.1 M HCl and extracted into ethyl acetate. TLC (eluent: 19:1 hexane/EtOAc) was used to confirm the consumption of the acyl chloride and therefore reaction completion (**2** R_f = 0.83; **3** R_f = 0.71). Upon completion, the reaction mixture was cooled to 0 °C. Deionized water (50 mL) was added in portions. The reaction was stirred for 5 min followed by the addition of ethanol (190 proof) (100 mL) and HCl (5 M, 200 mL) upon which the solution turned yellow. The reaction was stirred for 15 min, and then the white precipitates were collected via vacuum filtration and rinsed with hexane until no yellow color remained. The white solids were dried in vacuo overnight. Yield = 42.23 g (91%). ^{1}H NMR ($CDCl_3$, 400 MHz): δ 7.48 (t, 1H), 7.12 (d, 2H), 6.91 (s, 4H), 2.31 (s, 6H), 2.06 (s, 12H), 1.73 (s, 3H). $^{13}C\{^1H\}$ NMR ($CDCl_3$, 101 MHz): δ 204.4, 141.9, 137.7, 137.3, 136.6, 136.3, 129.3, 128.8, 128.2, 30.1, 21.2, 20.7. Major peaks (ν, cm^{-1}): 2967 (w), 2915 (w), 2855 (w), 1580 (m), 1484 (w), 1446 (s), 1375 (m), 1267 (m), 1103 (w), 1029 (m), 954 (w), 846 (s), 820 (m), 760 (s). Mp > 260 °C (limit of instrument). HRMS (ESI-TOF), m/z: $[M + H]^+$ Calcd for $C_{26}H_{28}O$ 357.2218; Found 357.2208.

Synthesis of Lithium 1-(2,6-Dimesitylphenyl)-1-ethenolate (4). To an oven-dried, nitrogen-filled 2 L round-bottom flask containing a PTFE-coated, magnetic stir bar and a reflux condenser were charged **3** (101 g, 283 mmol) and benzene (500 mL). *n*-BuLi (2.5 M in hexanes, 400 mL, 286.1 mmol) was cannulated into the reaction flask while stirring. The reaction solution turned dark brown and was set to reflux at 85 °C for 16 h. Benzene was removed via vacuum distillation. The remaining solids were pumped into the glovebox, slurried into hexane (200 mL) and collected via vacuum filtration. Solids were rinsed with minimal hexane and dried under vacuum to yield **4** as an off-white powder (92.8 g, 77% conversion to enolate determined by ^{1}H NMR). The product was used in the synthesis of H(**L**) without subsequent purification.

Synthesis of Bis(2,6-dimesitylbenzoyl)methane [H(L)]. In a nitrogen-filled glovebox, to a 500 mL round-bottom flask equipped with a stir bar and septum was charged a solution of **1** (48.56 g, 99 mmol) in CH_2Cl_2 (300 mL). **4** (92.8 g, 77% purity, 198 mmol) was added in portions. The solution was stirred at ambient temperature for 4 days. The flask was removed from the glovebox, and the contents were quenched with deionized water (10 mL), followed by 1 M HCl (100 mL) and 5 M HCl (100 mL) and stirred for 30 min. The layers were separated, and the aqueous layer was extracted with CH_2Cl_2 (50 mL). The organic layers were combined, concentrated, and slurried into acetone (100 mL) at 0 °C. The solids were filtered and washed with acetone until the filtrate appeared colorless, followed by the addition of portions of hexane. This crude powder was purified by column chromatography (dry loading, isocratic 15% CH_2Cl_2/hexane). H(**L**) was isolated as a colorless, crystalline solid. Yield = 48.3 g (70%). Additionally, **3** (55 g, 154 mmol) was recovered, giving an efficiency of 82% in *m*-terphenyl for the reaction. ^{1}H NMR ($CDCl_3$, 400 MHz): δ 16.11 (s, 1H), 7.36 (t, J = 7.6 Hz, 2H), 6.95 (d, J = 7.6 Hz, 4H), 6.78 (s, 8H), 4.80 (s, 1H), 2.26 (s, 12H), 1.75 (s, 24H). $^{13}C\{^1H\}$ NMR ($CDCl_3$, 101 MHz): δ 188.5, 140.2, 137.9, 136.4, 136.1, 135.8, 129.8, 129.7, 129.2, 128.4, 128.0, 125.4, 102.8, 21.3, 20.9. Major peaks (ν, cm^{-1}): 2938 (w), 2916 (m), 286 (w), 1585 (s), 1441 (s), 1373 (s), 1263 (m), 1023 (m), 845 (s), 759 (s). UV−vis (CH_2Cl_2): $\lambda_{max}(\varepsilon)$ 307 nm (5,690 M^{-1} cm^{-1}), 335 nm (6,090 M^{-1} cm^{-1}). Mp > 260 °C (limit of instrument). HRMS (ESI/Q-TOF), m/z: $[M + H]^+$ Calcd for $C_{51}H_{52}O_2$ 697.4045; Found 697.4030.

Synthesis of [Li(L)]$_2$. To an oven-dried 100 mL round-bottom flask equipped with a stir bar and a septum were charged H(**L**) (6.97 g, 10 mmol) and pentane (25 mL). *n*-BuLi, 2.5 M (4.4 mL, 11 mmol), is added via syringe, and the color rapidly transitions from purple to red to green. The mixture is allowed to stir at ambient temperature for 16 h. The product is filtered and washed with pentane to yield title compound as an off-white solid. Yield = 6.63 g (89%). Unreacted starting material is recovered from the filtrate by quenching with water and stirring in acetone. ^{1}H NMR (400 MHz, benzene-d_6) δ: 7.00 (s, 2H), 6.79 (s, 12H), 5.22 (s, 1H), 2.22 (s, 12H), 1.89 (s, 24H). Attempts to crystallize the material for XRD analysis repeatedly led to scavenging of THF from the glovebox, resulting in the determined structure of Li(**L**)(THF)$_2$ **5**.

Synthesis of [K(L)]$_2$ (6). In a nitrogen-filled glovebox, to a 100 mL round-bottom flask equipped with a stir bar and septum were charged H(**L**) (3.49 g, 5 mmol), KH (400 mg, 10 mmol), and 1:1 THF/toluene (30 mL). The contents were heated to 50 °C for 1 h. The flask was cooled to an ambient temperature. The light-brown slurry was vacuum filtered, and the solids were rinsed with toluene until only residual KH remained (gray solids) in the frit. The KH was quenched with *i*-PrOH in the ambient atmosphere. The filtrate was concentrated, and the crude solids were triturated in pentane (30 mL). The solids were collected via vacuum filtration to give [K(**L**)]$_2$ **6** as an off-white powder. Yield = 3.20 g (87%). ^{1}H NMR ($CDCl_3$, 400 MHz): δ 7.16 (t, J = 7.5 Hz, 2H), 6.85 (s, 4H), 6.75−6.67 (m, 8H), 4.63 (s, 1H), 2.38 (s, 12H), 1.94 (s, 12H), 1.71 (s, 12H). $^{13}C\{^1H\}$ NMR ($CDCl_3$, 101 MHz): δ 187.2, 144.1, 140.4, 137.9, 135.6, 134.9, 129.1, 129.0, 128.3, 127.3, 127.0, 126.6, 125.3, 102.0, 77.4, 77.1, 76.7, 22.0, 21.5, 21.3, 21.0. Major peaks (ν, cm^{-1}): 1610 (w), 1582 (m), 1560 (m), 1484 (w), 1427 (s), 1403 (s), 1371 (m), 1190 (w), 1026 (w), 850 (s), 768 (m), 734 (s). UV−vis (CH_2Cl_2): $\lambda_{max}(\varepsilon)$ 342 nm (23,500 M^{-1} cm^{-1}). Unreacted starting material was recovered as a white powder from the filtrate by being quenched with water and stirred in acetone and vacuum filtration.

Synthesis of [Tl(L)]$_2$ (7). In a nitrogen-filled glovebox, to a 100 mL round-bottom flask with a stir bar and septum were charged H(**L**) (3.0 g, 4.3 mmol) and THF (50 mL), and the contents were stirred to form a clear solution. TlOEt (0.3 mL, 4.3 mmol) was added via a syringe, turning the solution bright yellow. The reaction was stirred at ambient temperature for 1 h and then the solvent was removed under vacuum to yield [Tl(**L**)]$_2$ **7** as a pale-yellow powder. Yield = 3.6 g (93%). ^{1}H NMR ($CDCl_3$, 300 MHz): δ 7.22 (t, J = 7.5 Hz, 2H), 6.87 (d, J = 7.5 Hz, 4H), 6.76 (s, 8H), 4.60 (s, 1H), 2.27 (s, 12H), 1.80 (s, 24H). $^{13}C\{^1H\}$ NMR ($CDCl_3$, 101 MHz): δ 187.8, 143.5, 139.3, 137.9, 136.8, 136.0, 128.9, 127.8, 127.3, 103.7, 21.2. Major peaks (ν, cm^{-1}): 1610 (w), 1582 (m), 1560 (m), 1485 (m), 1423 (s), 1399 (s), 1373 (m), 1185 (w), 1121 (w), 1027 (w), 848 (s), 769 (m), 735 (s).

Synthesis of [Fe(L)(THF)(μ-Cl)$_2$]$_2$ (8). In a nitrogen-filled glovebox, a 350 mL bomb flask containing a PTFE-coated magnetic stir bar was charged with [K(**L**)]$_2$ **6** (1.6 g, 2.18 mmol), anhydrous $FeCl_2$ (304 mg, 2.39 mmol), and anhydrous THF (10 mL). The bomb flask was sealed under a reduced pressure. The mixture was heated at 90 °C for 3 days. The resulting orange solution was cooled to room temperature and vacuum filtered to remove KCl precipitates. Precipitates were washed with THF until only an off-white color remained. The filtrate was concentrated under vacuum. The resulting orange powder was slurried into CH_2Cl_2 (10 mL) and vacuum filtered to remove any remaining $FeCl_2$. The filtrate was concentrated to give

https://doi.org/10.1021/acs.inorgchem.4c03477
Inorg. Chem. 2024, 63, 23158−23168

$[Fe(\mathbf{L})(THF)(\mu\text{-}Cl)_2]_2$ **8** as a bright orange powder. Yield = 1.33 g (71%). IR (solid in Parabar oil, cm^{-1}): 2977 (w), 1614 (w), 1585 (m), 1510 (w), 1491 (s), 1439 (s), 1339 (m), 1275 (m), 1071 (s), 1037 (s), 851 (s), 780 (m), 765 (s), 747 (m). UV−vis (THF): λ_{max} (ε) 470 nm (340 M^{-1} cm^{-1}), 454 nm (350 M^{-1} cm^{-1}), 337 nm (29,000 M^{-1} cm^{-1}), 307 nm (27,000 M^{-1} cm^{-1}). μ_{eff} = 9.81(3) (Evans' Method, C_6D_6, 25 °C).

Synthesis of [Co(L)(THF)(μ-Cl)$_2$]$_2$ (9). In a nitrogen-filled glovebox, a 350 mL bomb flask containing a PTFE-coated magnetic stir bar was charged with $[K(\mathbf{L})]_2$ **6** (367 mg, 0.5 mmol), anhydrous $CoCl_2$ (195 mg, 1.5 mmol), and THF (3 mL). The bomb flask was sealed under reduced pressure and heated to 90 °C for 3 days. The dark teal solution was cooled to room temperature. The solids were filtered in the glovebox, and slow evaporation of the solvent afforded crystals of $[Co(\mathbf{L})(THF)(\mu\text{-}Cl)_2]_2$ **9** as dark teal blocks. Yield = 254 mg (40%). IR (solid in Parabar oil, cm^{-1}): 2989 (w), 1614 (w), 1580 (m), 1547 (s), 1510 (s), 1491 (s), 1439 (m), 1357 (s), 1275 (m), 1185 (w), 1036 (s), 944 (w), 913 (w), 883 (w), 842 (s), 760 (s). UV−vis (THF): λ_{max} (ε) 668 nm (320 M^{-1} cm^{-1}), 587 (180 M^{-1} cm^{-1}), 515 (120 M^{-1} cm^{-1}), 336 (27,000 M^{-1} cm^{-1}), 306 (23,000 M^{-1} cm^{-1}). μ_{eff} = 4.30 (Evans' Method, $CDCl_3$, 25 °C).

Synthesis of Co(L)(Cl)(MeCN) (12). In a nitrogen-filled glovebox, crystals of $[Co(\mathbf{L})(\mu\text{-}Cl)_2]_2$ **13** were dried to a powder under reduced pressure. The teal powder was crystallized via slow CH_3CN evaporation at room temperature to yield $Co(\mathbf{L})(Cl)(MeCN)$ **12** as dark purple crystals. IR (solid in Parabar oil, cm^{-1}): 2999.4 (w), 2322 (w), 2292 (w), 1614 (w), 1581 (m), 1529 (s), 1499 (s), 1447 (s), 1354 (s), 1037 (m), 855 (s), 829 (m), 780 (s), 747 (m). UV−vis (CH_3CN): λ_{max} (ε) 650 (312 M^{-1} cm^{-1}) 526 (294 M^{-1} cm^{-1}), 342 (32,000 M^{-1} cm^{-1}), 301 (25,000 M^{-1} cm^{-1}). μ_{eff} = 3.96 (Evans' Method, $CDCl_3$, 25 °C).

Synthesis of [Co(L)(μ-Cl)$_2$]$_2$ (13). In a nitrogen-filled glovebox, crystals of $[Co(\mathbf{L})(THF)(\mu\text{-}Cl)_2]_2$ **9** were dried to a powder under reduced pressure. The teal powder was crystallized via $CHCl_3$/toluene vapor diffusion to yield $[Co(\mathbf{L})(\mu\text{-}Cl)_2]_2$ **13**. IR (solid in Parabar oil, cm^{-1}): 2990 (w), 1614 (w), 1585 (m), 1551 (m), 1510 (s), 1495 (s), 1443 (m), 1361 (m), 1343 (m), 1279 (w), 1190 (w), 1074 (s), 1041 (w), 944 (w), 914 (w), 888 (w), 851 (s), 780 (m), 765 (m), 698 (m). μ_{eff} = 5.38 (Evans' Method, $CDCl_3$, 25 °C).

Synthesis of [Ni(L)(THF)(μ-Cl)]$_2$ (×10). In a nitrogen-filled glovebox, a 350 mL bomb flask containing a PTFE-coated magnetic stir bar was charged with $[K(\mathbf{L})]_2$ **6** (1 g, 1.36 mmol), anhydrous $NiCl_2$·dme (359 mg, 0.33 mmol), and 1:1 THF/dme (4 mL). The bomb flask was sealed under reduced pressure. The solution was heated to 90 °C for 3 days. The resulting yellow solution was cooled to room temperature and vacuum filtered in a nitrogen glovebox. Yellow precipitates were washed with THF. The yellow powder was slurried into dry $CHCl_3$ (10 mL) and vacuum filtered to remove any remaining KCl or $NiCl_2$·dme precipitates. The filtrate was dried to give $[Ni(\mathbf{L})(THF)(\mu\text{-}Cl)_2]_2$ **10** as a yellow powder. Yield = 130 mg (27%). IR (solid in Parabar oil, cm^{-1}): 2988 (w), 1614 (w), 1585 (m), 1551 (s), 1510 (m), 1495 (m), 1443 (m), 1365 (s), 1279 (w), 1190 (w), 1130 (w), 1041 (s), 848 (s), 892 (m), 851 (s), 825 (m), 776 (m), 698 (m). UV−vis ($CHCl_3$): λ_{max} (ε) 473(1400 M^{-1} cm^{-1}), 427 (1700 M^{-1} cm^{-1}), 344 (53,000 M^{-1} cm^{-1}), 294 (51,000 M^{-1} cm^{-1}). μ_{eff} = 4.10 (Evans' Method, $CDCl_3$, 25 °C).

Synthesis of [Ni(L)(μ-Cl)$_2$(THF)(H$_2$O)]$_2$ (14). The resulting yellow powder $[Ni(\mathbf{L})(THF)(\mu\text{-}Cl)_2]_2$ **10** was dissolved into $CHCl_3$ (hydrous, 10 mL). The resulting light green solution formed crystals of $[Ni(\mathbf{L})(\mu\text{-}Cl)_2(THF)(H_2O)]_2$ **14** via slow evaporation of solvent at room temperature. IR (solid in Parabar oil, cm^{-1}): 3005 (w), 1653 (w), 1610 (m), 1580 (s), 1551 (m), 1521 (m), 1507 (m), 1484 (m), 1437 (s), 1372 (s), 1270 (m), 1202 (m), 1031 (m), 848 (s), 821 (m), 774 (m), 760 (s), 744 (m). UV−vis (CH_2Cl_2): λ_{max} (ε) 462 (23 M^{-1} cm^{-1}), 653 (120 M^{-1} cm^{-1}). μ_{eff} = 5.6 (Evans' Method, $CDCl_3$, 25 °C).

Synthesis of [Cu(L)(μ-Cl)$_2$]$_2$ (11). In a nitrogen-filled glovebox, to a 100 mL round-bottom flask with a stir bar were added $[K(\mathbf{L})]_2$ **6** (2.21 g, 3 mmol), $CuCl_2$ (0.807 g, 6 mmol), and THF (25 mL). The dark green solution was stirred at room temperature for 16 h, upon which orange precipitates were vacuum filtered. The dark green filtrate was concentrated and recrystallized from hot toluene. Dark brown crystals were collected via vacuum filtration, rinsed with hexanes, and dried to give $[Cu(\mathbf{L})(\mu\text{-}Cl)]_2$ **11** as a light brown powder. Yield = 0.95 g (38%). IR (solid in Parabar oil, cm^{-1}): 3000.5 (w), 1610 (w), 1580 (w), 1491 (s), 1439 (s), 1375 (w), 1327 (s), 1182 (w), 1033 (m), 943 (w), 780 (m), 846 (s), 816 (m), 760 (s), 731 (m). UV−vis (CH_2Cl_2): λ_{max} (ε) 314 nm (25,000 M^{-1} cm^{-1}), 351 nm (30,200 M^{-1} cm^{-1}), 767 nm (240 M^{-1} cm^{-1}). μ_{eff} = 2.8 (Evans' Method, $CDCl_3$, 25 °C).

Synthesis of [Cu(L)(μ-OH)$_2$]$_2$ (15). Single crystals of **15** were grown by the slow evaporation of **16** from $CDCl_3$ under an ambient atmosphere.

Synthesis of [Cu(L)]$_2$ (16). In a nitrogen-filled glovebox, to a 20 mL vial equipped with a stir bar and a cap were charged $[Tl(\mathbf{L})]_2$ **7** (450 mg, 0.5 mmol), CuCl (200 mg, 2 mmol), and toluene (10 mL), and then the contents were stirred at ambient temperature for 1 h. The solution was filtered, and the solvent was removed in vacuo to give $[Cu(\mathbf{L})]_2$ **16** as a staticky yellow powder. Yield = 286 mg (75%). ^{1}H NMR (400 MHz, CDCl3) δ: 7.27 (t, 2H), 6.81 (d, 4H), 6.70 (s, 8H), 5.08 (s, 1H), 2.32 (s, 6H), 1.68 (s, 6H), 1.64 (s, 6H). 13C{1H} NMR (CDCl3, 101 MHz): δ 187.97, 143.21, 139.30, 137.84, 136.73, 135.87, 129.07, 128.88, 128.26, 127.72, 127.26, 125.34, 103.56, 77.37, 77.05, 76.73, 21.13, 21.11. IR (solid in Parabar oil, cm^{-1}): 3004 (w), 1610 (w), 1576 (w), 1535 (m), 1480 (m), 1431 (m), 1349 (s), 1271 (w), 1162 (w), 1122 (w), 1066 (w), 1025 (w), 846.1 (s), 768 (m), 746 (m).

■ ASSOCIATED CONTENT

Supporting Information

The Supporting Information is available free of charge at https://pubs.acs.org/doi/10.1021/acs.inorgchem.4c03477.

Experimental details, methods, and characterization including ^{1}H NMR, ^{13}C NMR, HRMS, IR, UV−vis, and sc-XRD for characterized compounds are provided (PDF)

Accession Codes

CCDC 2350939−2350951 contain the supplementary crystallographic data for this paper. These data can be obtained free of charge via www.ccdc.cam.ac.uk/data_request/cif,orby emailing data_request@ccdc.cam.ac.uk, or by contacting The Cambridge Crystallographic Data Centre, 12 Union Road, Cambridge CB2 1EZ, UK; fax: + 44 1223 336033.

■ AUTHOR INFORMATION

Corresponding Authors

Michael P. Marshak − *Department of Chemistry, University of Wyoming, Laramie, Wyoming 82071, United States;* orcid.org/0000-0002-8027-2705; Email: mmarshak@uwyo.edu

Aaron S. Crossman − *Department of Chemistry, University of Colorado Boulder, Boulder, Colorado 80309, United States;* Present Address: Bedoukian Research, Inc., 6 Commerce Dr., Danbury, CT 06810; acrossman@bedoukian.com; orcid.org/0000-0001-9228-4116; Email: acrossman@protonmail.com

Authors

Claire E. Boronski − *Department of Chemistry, University of Colorado Boulder, Boulder, Colorado 80309, United States*

Sebastian M. Krajewski − *Department of Chemistry, University of Colorado Boulder, Boulder, Colorado 80309, United States;* orcid.org/0000-0002-9755-2375

Erin E. Sanchez − *Department of Chemistry, University of Colorado Boulder, Boulder, Colorado 80309, United States*

Complete contact information is available at:
https://pubs.acs.org/10.1021/acs.inorgchem.4c03477

Author Contributions

Experimental work conducted by A.S.C. and C.E.B. Routine synthesis performed by E.E.S. Crystallographic analyses by C.E.B and S.M.K. Computational work conducted by A.S.C. with assistance from C.E.B. The manuscript was prepared by A.S.C. and C.E.B., and all authors have given approval to the final version.

Funding

The work presented herein was funded by the National Science Foundation under Grant No. 2155227 and by laboratory startup funds provided by the University of Colorado, Boulder.

Notes

The authors declare the following competing financial interest(s): Michael Marshak has patent US9676693B2 issued to Michael Marshak.

■ ABBREVIATIONS

scXRD, single-crystal X-ray diffraction
acac, acetylacetenoate
NacNac, 1,3-diketimine
THF, tetrahydrofuran
DFT, density functional theory
IR, infrared spectroscopy
UV−vis, ultraviolet−visible spectroscopy
NMR, nuclear magnetic resonance
HRMS, high resolution mass spectrometry

■ REFERENCES

(1) Miyaura, N.; Yamada, K.; Suzuki, A. A New Stereospecific Cross-Coupling by the Palladium-Catalyzed Reaction of 1-Alkenylboranes with 1-Alkenyl or 1-Alkynyl Halides. *Tetrahedron Lett.* **1979**, *20* (36), 3437−3440.
(2) Sonogashira, K.; Tohda, Y.; Hagihara, N. A Convenient Synthesis of Acetylenes: Catalytic Substitutions of Acetylenic Hydrogen with Bromoalkenes, Iodoarenes and Bromopyridines. *Tetrahedron Lett.* **1975**, *16* (50), 4467−4470.
(3) Paul, F.; Patt, J.; Hartwig, J. F. Palladium-Catalyzed Formation of Carbon-Nitrogen Bonds. Reaction Intermediates and Catalyst Improvements in the Hetero Cross-Coupling of Aryl Halides and Tin Amides. *J. Am. Chem. Soc.* **1994**, *116* (13), 5969−5970.
(4) Guram, A. S.; Buchwald, S. L. Palladium-Catalyzed Aromatic Aminations with in Situ Generated Aminostannanes. *J. Am. Chem. Soc.* **1994**, *116* (17), 7901−7902.
(5) Hayler, J. D.; Leahy, D. K.; Simmons, E. M. A Pharmaceutical Industry Perspective on Sustainable Metal Catalysis. *Organometallics* **2019**, *38* (1), 36−46.
(6) Blakemore, D. C.; Castro, L.; Churcher, I.; Rees, D. C.; Thomas, A. W.; Wilson, D. M.; Wood, A. Organic Synthesis Provides Opportunities to Transform Drug Discovery. *Nat. Chem.* **2018**, *10* (4), 383−394.
(7) Brown, D. G.; Boström, J. Analysis of Past and Present Synthetic Methodologies on Medicinal Chemistry: Where Have All the New Reactions Gone? *J. Med. Chem.* **2016**, *59* (10), 4443−4458.
(8) Surry, D. S.; Buchwald, S. L. Dialkylbiaryl Phosphines in Pd-Catalyzed Amination: A User's Guide. *Chem. Sci.* **2011**, *2* (1), 27−50.
(9) Mindiola, D. J. Nacnac ... Are You Still There? The Evolution of β-Diketiminate Complexes of Nickel. *Angew. Chem., Int. Ed.* **2009**, *48* (34), 6198−6200.
(10) Camp, C.; Arnold, J. On the Non-Innocence of "Nacnacs": Ligand-Based Reactivity in β-Diketiminate Supported Coordination Compounds. *Dalton Transactions* **2016**, *45* (37), 14462−14498.
(11) Przyojski, J. A.; Arman, H. D.; Tonzetich, Z. J. Complexes of Iron(II) and Iron(III) Containing Aryl-Substituted N-Heterocyclic Carbene Ligands. *Organometallics* **2012**, *31* (8), 3264−3271.
(12) Arduengo, A. J., III; Dias, H. V. R.; Calabrese, J. C.; Davidson, F. Homoleptic Carbene-Silver(1) and Carbene-Copper(1) Complexes. *Organometallics* **1993**, *12* (9), 3405−3409.
(13) Hopkins, E. J.; Krajewski, S. M.; Crossman, A. S.; Maharaj, F. D. R.; Schwanz, L. T.; Marshak, M. P. Group 4 Organometallics Supported by Sterically Hindered β -Diketonates: Group 4 Organometallics Supported by Sterically Hindered β -Diketonates. *Eur. J. Inorg. Chem.* **2020**, *2020* (20), 1951−1959.
(14) Carroll, T. G.; Ryan, D. E.; Erickson, J. D.; Bullock, R. M.; Tran, B. L. Isolation of a Cu−H Monomer Enabled by Remote Steric Substitution of a N-Heterocyclic Carbene Ligand: Stoichiometric Insertion and Catalytic Hydroboration of Internal Alkenes. *J. Am. Chem. Soc.* **2022**, *144* (30), 13865−13873.
(15) Das, A.; Van Trieste, G. P., III; Powers, D. C. Crystallography of Reactive Intermediates. *Comments on Inorganic Chemistry* **2020**, *40* (3), 116−158.
(16) Spencer, D. J. E.; Aboelella, N. W.; Reynolds, A. M.; Holland, P. L.; Tolman, W. B. β-Diketiminate Ligand Backbone Structural Effects on Cu(I)/O2 Reactivity: Unique Copper−Superoxo and Bis(μ-Oxo) Complexes. *J. Am. Chem. Soc.* **2002**, *124* (10), 2108−2109.
(17) Kleeberg, C.; Borner, C. Syntheses, Structures, and Reactivity of NHC Copper(I) Boryl Complexes: A Systematic Study. *Organometallics* **2018**, *37* (21), 4136−4146.
(18) Gentner, T. X.; Rösch, B.; Ballmann, G.; Langer, J.; Elsen, H.; Harder, S. Low Valent Magnesium Chemistry with a Super Bulky β-Diketiminate Ligand. *Angew. Chem.* **2019**, *131* (2), 617−621.
(19) Kays, D. L. Extremely Bulky Amide Ligands in Main Group Chemistry. *Chem. Soc. Rev.* **2016**, *45* (4), 1004−1018.
(20) Pakiam, R. Palladium Smashes $1,500 as Shortages Ignite Record-Breaking Rally. *Bloomberg*. February 19, 2019. https://www.bloomberg.com/news/articles/2019-02-20/palladium-tops-1-500-as-shortages-ignite-record-breaking-rally (accessed 2019-07-11).
(21) Chirik, P.; Morris, R. Getting Down to Earth: The Renaissance of Catalysis with Abundant Metals. *Acc. Chem. Res.* **2015**, *48* (9), 2495−2495.
(22) Czaplik, W. M.; Mayer, M.; Cvengroš, J.; von Wangelin, A. J. Coming of Age: Sustainable Iron-Catalyzed Cross-Coupling Reactions. *ChemSusChem* **2009**, *2* (5), 396−417.
(23) Piontek, A.; Bisz, E.; Szostak, M. Iron-Catalyzed Cross-Couplings in the Synthesis of Pharmaceuticals: In Pursuit of Sustainability. *Angew. Chem., Int. Ed.* **2018**, *57* (35), 11116−11128.
(24) Holland, P. L. Reaction: Opportunities for Sustainable Catalysts. *Chem.* **2017**, *2* (4), 443−444.
(25) *Metal Sustainability: Global Challenges, Consequences, and Prospects*; Izatt, R. M., Ed.; John Wiley & Sons, Ltd.: Chichester, UK, 2016; DOI: 10.1002/9781119009115.
(26) Sherry, B. D.; Fürstner, A. The Promise and Challenge of Iron-Catalyzed Cross Coupling. *Acc. Chem. Res.* **2008**, *41* (11), 1500−1511.
(27) Fischer, E.; Bülow, C. Ueber das Benzoylaceton. *Reports of the German Chemical Society* **1885**, *18* (2), 2131−2138.
(28) Combes, M. A. Nouvelle reaction du chlorure d'aluminium, syntheses dans la serie grasse. *Compt Rend* **1886**, *103*, 814−817.
(29) Claisen, L. Ueber die Einführung von Säureradicalen in Ketone. *Berichte der deutschen chemischen Gesellschaft* **1887**, *20* (1), 655−657.
(30) Combes, A. Sur les derives metalliques de l'acetylacetone. *Comptes rendus hebdomadaires des séances de l'Académie des sciences* **1887**, *105*, 868−871.
(31) Johnson, J. Y. Farbenindustrie Aktiengesellschaft. Improvements in the Catalytic Oxidation of Organic Compounds. GB303268A, January 3, 1929.
(32) Larson, A. T.; Crossman, A. S.; Krajewski, S. M.; Marshak, M. P. Copper(II) as a Platform for Probing the Steric Demand of Bulky β-Diketonates. *Inorg. Chem.* **2020**, *59* (1), 423−432.

(33) Al-Anbar, M.; Daoud, H. Synthesis and Characterization of Metal-Beta-Diketonate Coordination Complexes and Polymers. *Oriental Journal Of Chemistry* **2013**, *29*, 905−909.
(34) Toscano, P. J.; Dettelbacher, C.; Waechter, J.; Pavri, N. P.; Hunt, D. H.; Eisenbraun, E. T.; Zheng, B.; Kaloyeros, A. E. SYNTHESIS AND CHARACTERIZATION OF POLYFLUORINATED β-DIKETONATE TRANSITION METAL COMPLEXES1,2. *J. Coord. Chem.* **1996**, *38* (4), 319−335.
(35) Krajewski, S. M.; Crossman, A. S.; Akturk, E. S.; Suhrbier, T.; Scappaticci, S. J.; Staab, M. W.; Marshak, M. P. Sterically Encumbered β-Diketonates and Base Metal Catalysis. *Dalton Trans* **2019**, *48* (28), 10714−10722.
(36) Fatta, A. M.; Lintvedt, R. L. Nephelauxetic and Spectrochemical Series for 1,3-Diketonates. Ligand Field Spectra of Some Tris(1,3-Diketonato)Chromium(III) Chelates. *Inorg. Chem.* **1971**, *10* (3), 478−481.
(37) Schäffer, C. E.; Klixbüll Jørgensen, C. The Nephelauxetic Series of Ligands Corresponding to Increasing Tendency of Partly Covalent Bonding. *Journal of Inorganic and Nuclear Chemistry* **1958**, *8*, 143−148.
(38) Mehrotra, R. C.; Bohra, R.; Gaur, D. P. *Metal B-Diketonates and Allied Derivatives*; Academic Press, 1978.
(39) Crossman, A. S.; Marshak, M. P. Beta-Diketones: Coordination and Application. *Comprehensive Coordination Chemistry*; Elsevier, 2021; p 6000.
(40) Fernandes, G. F. S.; Pontes, M. A. P.; Machado, F. B. C.; Ferrão, L. F. A. Electronic Structure and Stability of Transition Metal Acetylacetonates TM(AcAc)n (TM = Cr, Fe, Co, Ni, Cu; n = 1, 2, 3). *Computational and Theoretical Chemistry* **2022**, *1207*, No. 113502.
(41) Jørgensen, Chr. K. The Nephelauxetic Series. *Prog. Inorg. Chem.*, Vol. *4*; John Wiley & Sons, Ltd., 1962; pp 73−124, DOI: 10.1002/9780470166055.ch2.
(42) Chan, J. C. C.; Au-Yeung, S. C. F. Interpretation of 59Co NMR Shielding Using the Hard and Soft Acid−Base Concept. Insight into the Relative Magnitude of the Nephelauxetic and the Spectrochemical Effect. *J. Chem. Soc., Faraday Trans.* **1996**, *92* (7), 1121−1128.
(43) Crossman, A. S.; Larson, A. T.; Shi, J. X.; Krajewski, S. M.; Akturk, E. S.; Marshak, M. P. Synthesis of Sterically Hindered β-Diketones via Condensation of Acid Chlorides with Enolates. *J. Org. Chem.* **2019**, *84* (11), 7434−7442.
(44) Campeau, L.-C.; Hazari, N. Cross-Coupling and Related Reactions: Connecting Past Success to the Development of New Reactions for the Future. *Organometallics* **2019**, *38* (1), 3−35.
(45) Fürstner, A.; Leitner, A.; Méndez, M.; Krause, H. Iron-Catalyzed Cross-Coupling Reactions. *J. Am. Chem. Soc.* **2002**, *124* (46), 13856−13863.
(46) Conradie, J. Bis(Acetylacetonato)Copper(II) − Structural and Electronic Data of the Neutral, Oxidized and Reduced Forms. *Data in Brief* **2019**, *26*, No. 104511.
(47) He, C.; Zhang, G.; Ke, J.; Zhang, H.; Miller, J. T.; Kropf, A. J.; Lei, A. Labile Cu(I) Catalyst/Spectator Cu(II) Species in Copper-Catalyzed C−C Coupling Reaction: Operando IR, in Situ XANES/EXAFS Evidence and Kinetic Investigations. *J. Am. Chem. Soc.* **2013**, *135* (1), 488−493.
(48) Ullmann, F.; Bielecki, J. Ueber Synthesen in der Biphenylreihe. *Ber. Dtsch. Chem. Ges* **1901**, *34* (2), 2174−2185.
(49) Shafir, A.; Buchwald, S. L. Highly Selective Room-Temperature Copper-Catalyzed C−N Coupling Reactions. *J. Am. Chem. Soc.* **2006**, *128* (27), 8742−8743.
(50) Beletskaya, I. P.; Cheprakov, A. V. Copper in Cross-Coupling Reactions The Post-Ullmann Chemistry. *Coord. Chem. Rev.* **2004**, *248* (21−24), 2337−2346.
(51) Jones, G. O.; Liu, P.; Houk, K. N.; Buchwald, S. L. Computational Explorations of Mechanisms and Ligand-Directed Selectivities of Copper-Catalyzed Ullmann-Type Reactions. *J. Am. Chem. Soc.* **2010**, *132* (17), 6205−6213.
(52) Krizewsky, J.; Turner, E. E. XLIV.—Formation of Diphenyl by the Action of Cupric Salts on Organometallic Compounds of Magnesium. *Journal of the Chemical Society, Transactions* **1919**, *115*, 559−561.
(53) Ebert, G.; Rieke, R. D. Direct Formation of Organocopper Compounds by Oxidative Addition of Zerovalent Copper to Organic Halides. *Journal of Organic Chemistry* **1984**, *49* (26), 5280−5282.
(54) Adams, J. T.; Hauser, C. R. The Acylation of Ketones with Aliphatic Anhydrides by Means of Boron Trifluoride. Synthesis of 8-Diketones. *J. Am. Chem. Soc.* **1945**, *67* (2), 284−286.
(55) Kopecky, K. R.; Nonhebel, D.; Morris, G.; Hammond, G. S. Preparation of Dipivaloylmethane. *Journal of Organic Chemistry* **1962**, *27* (3), 1036−1037.
(56) Bourget-Merle, L.; Lappert, M. F.; Severn, J. R. The Chemistry of β-Diketiminatometal Complexes. *Chem. Rev.* **2002**, *102* (9), 3031−3066.
(57) Complexes of Bulky β-Diketiminate Ligands. *Inorganic Syntheses*, Vol. *35*; John Wiley & Sons, Ltd., 2010; pp 1−55, DOI: 10.1002/9780470651568.ch1.
(58) Fan, H.; Adhikari, D.; Saleh, A. A.; Clark, R. L.; Zuno-Cruz, F. J.; Sanchez Cabrera, G.; Huffman, J. C.; Pink, M.; Mindiola, D. J.; Baik, M.-H. Understanding and Predicting Distorted T- versus Y-Geometries for Neutral Chromous Complexes Supported by a Sterically Encumbering β-Diketiminate Ligand. *J. Am. Chem. Soc.* **2008**, *130* (51), 17351−17361.
(59) Kundu, S.; Greene, C.; Williams, K. D.; Salvador, T. K.; Bertke, J. A.; Cundari, T. R.; Warren, T. H. Three-Coordinate Copper(II) Aryls: Key Intermediates in C−O Bond Formation. *J. Am. Chem. Soc.* **2017**, *139* (27), 9112−9115.
(60) Smith, J. M.; Lachicotte, R. J.; Holland, P. L. Three-Coordinate, 12-Electron Organometallic Complexes of Iron(II) Supported by a Bulky β-Diketiminate Ligand: Synthesis and Insertion of CO To Give Square-Pyramidal Complexes. *Organometallics* **2002**, *21* (22), 4808−4814.
(61) Parks, J. E.; Holm, R. H. Synthesis, Solution Stereochemistry, and Electron Delocalization Properties of Bis(.Beta.-Iminoamino)-Nickel(II) Complexes. *Inorg. Chem.* **1968**, *7* (7), 1408−1416.
(62) Chen, C.; Bellows, S. M.; Holland, P. L. Tuning Steric and Electronic Effects in Transition-Metal β-Diketiminate Complexes. *Dalton Trans* **2015**, *44* (38), 16654−16670.
(63) Do, D. C. H.; Keyser, A.; Protchenko, A. V.; Maitland, B.; Pernik, I.; Niu, H.; Kolychev, E. L.; Rit, A.; Vidovic, D.; Stasch, A.; Jones, C.; Aldridge, S. Highly Electron-Rich β-Diketiminato Systems: Synthesis and Coordination Chemistry of Amino-Functionalized " *N* -Nacnac" Ligands. *Chem.—Eur. J.* **2017**, *23* (24), 5830−5841.
(64) Basuli, F.; Huffman, J. C.; Mindiola, D. J. Reactivity at the β-Diketiminate Ligand Nacnac $^{-}$ on Titanium(IV) (Nacnac $^{-}$ = [Ar]NC(CH $_3$)CHC(CH $_3$)N[Ar], Ar = 2,6-[CH(CH $_3$) $_2$] $_2$ C $_6$ H $_3$). Diimine-Alkoxo and Bis-Anilido Ligands Stemming from the Nacnac $^{-}$ Skeleton. *Inorg. Chem.* **2003**, *42* (24), 8003−8010.
(65) MacAdams, L. A.; Kim, W.-K.; Liable-Sands, L. M.; Guzei, I. A.; Rheingold, A. L.; Theopold, K. H. The (Ph) $_2$ Nacnac Ligand in Organochromium Chemistry. *Organometallics* **2002**, *21* (5), 952−960.
(66) O'Neill, P. M.; Hindley, S.; Pugh, M. D.; Davies, J.; Bray, P. G.; Park, B. K.; Kapu, D. S.; Ward, S. A.; Stocks, P. A. Co(Thd)2: A Superior Catalyst for Aerobic Epoxidation and Hydroperoxysilylation of Unactivated Alkenes: Application to the Synthesis of Spiro-1,2,4-Trioxanes. *Tetrahedron Lett.* **2003**, *44* (44), 8135−8138.
(67) Altman, R. A.; Buchwald, S. L. Cu-Catalyzed *N* - and *O* -Arylation of 2-, 3-, and 4-Hydroxypyridines and Hydroxyquinolines. *Org. Lett.* **2007**, *9* (4), 643−646.
(68) Primer, D. N.; Molander, G. A. Enabling the Cross-Coupling of Tertiary Organoboron Nucleophiles through Radical-Mediated Alkyl Transfer. *J. Am. Chem. Soc.* **2017**, *139* (29), 9847−9850.
(69) Akturk, E. S.; Scappaticci, S. J.; Seals, R. N.; Marshak, M. P. Bulky β-Diketones Enabling New Lewis Acidic Ligand Platforms. *Inorg. Chem.* **2017**, *56* (19), 11466−11469.
(70) Crossman, A. S.; Shi, J. X.; Krajewski, S. M.; Maurer, L. A.; Marshak, M. P. Synthesis, Reactivity, and Crystallography of a Sterically Hindered Acyl Triflate. *Tetrahedron* **2021**, *94*, No. 132308.

(71) Effenberger, F. Electrophilic Reagents—Recent Developments and Their Preparative Application. *Angew. Chem., Int. Ed.* **1980**, *19* (3), 151−171.
(72) Addison, A. W.; Rao, T. N.; Reedijk, J.; van Rijn, J.; Verschoor, G. C. Synthesis, Structure, and Spectroscopic Properties of Copper(II) Compounds Containing Nitrogen−Sulphur Donor Ligands; the Crystal and Molecular Structure of Aqua[1,7-Bis(N-Methylbenzimidazol-2′-Yl)-2,6-Dithiaheptane]Copper(II) Perchlorate. *J. Chem. Soc., Dalton Trans.* **1984**, *7*, 1349−1356.
(73) Yang, L.; Powell, D. R.; Houser, R. P. Structural Variation in Copper(I) Complexes with Pyridylmethylamide Ligands: Structural Analysis with a New Four-Coordinate Geometry Index, T4. *Dalton Trans* **2007**, *9*, 955−964.
(74) Bhattacharjee, M. N.; Chaudhuri, M. K.; Ghosh, S. K.; Hiese, Z.; Roy, N. Direct Synthesis of Bis(Acetylacetonato)Nickel(II) Dihydrate and Isolation of $\alpha,\alpha,\beta,\beta$-Tetra-Acetylethane as the Oxidation Product of Acetylacetone. *J. Chem. Soc., Dalton Trans.* **1983**, *12*, 2561−2562.
(75) Gromilov, S. A.; Baidina, I. A. Regularities of Crystal Structures of Cu(II) β-Diketonates. *J. Struct Chem.* **2004**, *45* (6), 1031−1081.
(76) Irving, H.; Williams, R. J. P. 637. The Stability of Transition-Metal Complexes. *J. Chem. Soc.* **1953**, *0*, 3192−3210.
(77) *Software update: The ORCA program system—Version 5.0 - Neese - 2022 - WIREs Computational Molecular Science - Wiley Online Library*. https://wires.onlinelibrary.wiley.com/doi/10.1002/wcms.1606 (accessed 2024-04-24).
(78) Shibata, S.; Onuma, S.; Iwase, A.; Inoue, H. The Crystal Structure of Dimeric Bis(Acetylacetonato)Iron(II). *Inorg. Chim. Acta* **1977**, *25*, 33−39.
(79) Cotton, F. A.; Elder, R. C. Crystal Structure of Tetrameric Cobalt(II) Acetylacetonate. *Inorg. Chem.* **1965**, *4* (8), 1145−1151.
(80) Bullen, G. J.; Mason, R.; Pauling, P. The Crystal and Molecular Structure of Bis(Acetylacetonato)Nickel (II). *Inorg. Chem.* **1965**, *4* (4), 456−462.
(81) Boonseng, S.; Roffe, G. W.; Targema, M.; Spencer, J.; Cox, H. Rationalization of the Mechanism of *in Situ* Pd(0) Formation for Cross-Coupling Reactions from Novel Unsymmetrical Pincer Palladacycles Using DFT Calculations. *J. Organomet. Chem.* **2017**, *845*, 71−81.
(82) Fraile, J. M.; García, J. I.; Martínez-Merino, V.; Mayoral, J. A.; Salvatella, L. Theoretical (DFT) Insights into the Mechanism of Copper-Catalyzed Cyclopropanation Reactions. Implications for Enantioselective Catalysis. *J. Am. Chem. Soc.* **2001**, *123* (31), 7616−7625.
(83) Bellows, S. M.; Arnet, N. A.; Gurubasavaraj, P. M.; Brennessel, W. W.; Bill, E.; Cundari, T. R.; Holland, P. L. The Mechanism of N−N Double Bond Cleavage by an Iron(II) Hydride Complex. *J. Am. Chem. Soc.* **2016**, *138* (37), 12112−12123.
(84) Spencer, D. J. E.; Reynolds, A. M.; Holland, P. L.; Jazdzewski, B. A.; Duboc-Toia, C.; Le Pape, L.; Yokota, S.; Tachi, Y.; Itoh, S.; Tolman, W. B. Copper Chemistry of β-Diketiminate Ligands: Monomer/Dimer Equilibria and a New Class of Bis(μ-Oxo)Dicopper Compounds. *Inorg. Chem.* **2002**, *41* (24), 6307−6321.
(85) Wiencko, H. L.; Kogut, E.; Warren, T. H. Neutral β-Diketiminato Nickel(II) Monoalkyl Complexes. *Inorg. Chim. Acta* **2003**, *345*, 199−208.
(86) Smith, R. S.; Kochi, J. K. Mechanistic Studies of Iron Catalysis in the Cross Coupling of Alkenyl Halides and Grignard Reagents. *J. Org. Chem.* **1976**, *41* (3), 502−509.
(87) Fürstner, A.; Leitner, A. Iron-Catalyzed Cross-Coupling Reactions of Alkyl-Grignard Reagents with Aryl Chlorides, Tosylates, and Triflates. *Angew. Chem., Int. Ed.* **2002**, *41* (4), 609−612.
(88) Weber, K.; Schnöckelborg, E.-M.; Wolf, R. Catalytic Properties of Low Oxidation State Iron Complexes in Cross-Coupling Reactions: Anthracene Iron(−I) Complexes as Competent Catalysts. *ChemCatChem.* **2011**, *3* (10), 1572−1577.
(89) Schoch, R.; Desens, W.; Werner, T.; Bauer, M. X-Ray Spectroscopic Verification of the Active Species in Iron-Catalyzed Cross-Coupling Reactions. *Chemistry − A European Journal* **2013**, *19* (47), 15816−15821.
(90) Heravi, M. M.; Zadsirjan, V.; Hajiabbasi, P.; Hamidi, H. Advances in Kumada−Tamao−Corriu Cross-Coupling Reaction: An Update. *Monatsh. Chem.* **2019**, *150* (4), 535−591.
(91) Tamura, M.; Kochi, J. K. Vinylation of Grignard Reagents. Catalysis by Iron. *J. Am. Chem. Soc.* **1971**, *93* (6), 1487−1489.
(92) Scappaticci, S. J.; Crossman, A. S.; Larson, A. T.; Maharaj, F. D. R.; Akturk, E. S.; Marshak, M. P. Mechanistic Investigation of Iron-Catalyzed Cross-Coupling Using Sterically Encumbered β-Diketonate Ligands. *Polyhedron* **2024**, *259*, No. 117027.
(93) Tamura, M.; Kochi, J. K. The Reactions of Grignard Reagents with Transition Metal Halides: Coupling, Disproportionation, and Exchange with Olefins. *BCSJ.* **1971**, *44* (11), 3063−3073.
(94) Sambiagio, C.; Marsden, S. P.; Blacker, A. J.; McGowan, P. C. Copper Catalysed Ullmann Type Chemistry: From Mechanistic Aspects to Modern Development. *Chem. Soc. Rev.* **2014**, *43* (10), 3525−3550.
(95) Yang, Q.; Zhao, Y.; Ma, D. Cu-Mediated Ullmann-Type Cross-Coupling and Industrial Applications in Route Design, Process Development, and Scale-up of Pharmaceutical and Agrochemical Processes. *Org. Process Res. Dev.* **2022**, *26* (6), 1690−1750.
(96) Monnier, F.; Taillefer, M. Catalytic C-C, C-N, and C-O Ullmann-Type Coupling Reactions. *Angew. Chem., Int. Ed.* **2009**, *48* (38), 6954−6971.
(97) Lefèvre, G.; Tlili, A.; Taillefer, M.; Adamo, C.; Ciofini, I.; Jutand, A. Discriminating Role of Bases in Diketonate Copper(i)-Catalyzed C−O Couplings: Phenol versus Diarylether. *Dalton Transactions* **2013**, *42* (15), 5348.
(98) Crossman, A. S.; Larson, A. T.; Shi, J. X.; Krajewski, S. M.; Akturk, E. S.; Marshak, M. P. Synthesis of Sterically Hindered β-Diketones via Condensation of Acid Chlorides with Enolates. *J. Org. Chem.* **2019**, *84* (11), 7434−7442.
(99) Evans, D. F. 400. The Determination of the Paramagnetic Susceptibility of Substances in Solution by Nuclear Magnetic Resonance. *J. Chem. Soc.* **1959**, *0* (0), 2003−2005.
(100) Bain, G. A.; Berry, J. F. Diamagnetic Corrections and Pascal's Constants. *J. Chem. Educ.* **2008**, *85* (4), 532.

https://doi.org/10.1021/acs.inorgchem.4c03477
Inorg. Chem. 2024, 63, 23158−23168